Available online at www.sciencedirect.com
ScienceDirect
Journal of Power Sources 160 (2006) 558–562
JOURNAL OF POWER SOURCES
www.elsevier.com/locate/jpowsour

Synthesis and characterization of spherical morphology $[Ni_{0.4}Co_{0.2}Mn_{0.4}]_3O_4$ materials for lithium secondary batteries

Sung Woo Oh [a], Sang-Ho Park [a,b], K. Amine [b], Yang-Kook Sun [a,*]

[a] *Center for Information and Communication Materials, Department of Chemical Engineering, Hanyang University, Seungdong-Gu, Seoul 133-791, Republic of Korea*
[b] *Argonne National Laboratory, 9700 S. Cass Ave., Argonne, IL 60439, USA*

Received 8 November 2005; received in revised form 3 January 2006; accepted 5 January 2006
Available online 17 February 2006

Abstract

Spherical morphology $[Ni_{0.4}Co_{0.2}Mn_{0.4}]_3O_4$ materials have been synthesized by ultrasonic spray pyrolysis. The $Li[Ni_{0.4}Co_{0.2}Mn_{0.4}]O_2$ powders were prepared at various pyrolysis temperatures between 500 and 900 °C. The $Li[Ni_{0.4}Co_{0.2}Mn_{0.4}]O_2$ material prepared at a pyrolysis temperature of 600 °C samples are exhibited excellent electrochemical cycling performance and delivered the highest discharge capacity at over 180 mAh g^{-1} between 2.8 and 4.4 V. The structural, electrochemical, morphological property and thermal stability of the powders were characterized by X-ray diffraction (XRD), galvanostatic charge/discharge testing, scanning electron microscopy (SEM), and differential scanning calorimeter (DSC), respectively.

Keywords: Lithium secondary batteries; Spray pyrolysis; Positive materials; Layered materials; Electrochemical properties

1. Introduction

Extensive research for alternatives to $LiCoO_2$ as the positive material in rechargeable batteries has been conducted over the past few years. Alternative cathode materials are being sought because $LiCoO_2$ is expensive and toxic. The promising alternatives include hexagonal α-$NaFeO_2$ structured-layered lithium transition metal oxides $LiMO_2$ (M = Co, Ni, Mn), particularly $LiNiO_2$ and $LiMnO_2$. Although there has been much progress in optimizing these two materials, there are still problems that need to be overcome. For example, $LiNiO_2$ cannot be used in its current form because stoichiometric $LiNiO_2$ is known to be difficult to synthesize and delithiated Li_xNiO_2 decomposes exothermally at around 200 °C [1–3]. $LiMnO_2$, on the other hand, is thermodynamically unstable as a layered structure, but thermodynamically stable as orthorhombic phase *o*-$LiMnO_2$ [4]. The Mn^{3+} (d^4) ions cause a cooperative distortion of the MnO_6 octahedral due to Jahn–Teller stabilization leading to a monoclinic unit cell. When Li is deintercalated from the $LiMnO_2$, both the *m*- and *o*-$LiMnO_2$ have been observed to undergo a detrimental phase transformation to a spinel-like phase through minor atomic rearrangements leading to eventual degradation of electrode performance [5,6].

Several recent attempts have been made to enhance the electrochemical performance of $LiNiO_2$–$LiCoO_2$–$LiMnO_2$ solid solution [7,8]. Among them, $Li[Ni_{1/3}Co_{1/3}Mn_{1/3}]O_2$ has been suggested as the most promising alternative to $LiCoO_2$ since Ni, Co, and Mn can substitute each other to form a solid solution of any percentage without disturbing the layer structure. Recently, we reported on the structural and electrochemical properties of $Li[Ni_{0.5}Mn_{0.5}]_{1-x}Co_xO_2$ (x in 0–0.33) materials [9].

In this study, we synthesized $[Ni_{0.4}Co_{0.2}Mn_{0.4}]O_y$ precursor at various pyrolysis temperatures in order to obtain optimized $Li[Ni_{0.4}Co_{0.2}Mn_{0.4}]O_2$ cathode materials. The structural and electrochemical properties of these cathode materials were investigated by X-ray diffraction and electrochemical measurements.

2. Experimental

$Li[Ni_{0.4}Co_{0.2}Mn_{0.4}]O_2$ powder was synthesized by a spray pyrolysis method. At first, stoichiometric amounts of nickel

* Corresponding author. Tel.: +82 2 2220 0524; fax: +82 2 2282 7329.
E-mail address: yksun@hanyang.ac.kr (Y.-K. Sun).

0378-7753/$ – see front matter © 2006 Elsevier B.V. All rights reserved.
doi:10.1016/j.jpowsour.2006.01.023

nitrate hexahydrate ($Ni(NO_3)\cdot 6H_2O$, Aldrich), cobalt nitrate hexahydrate ($Co(NO_3)_2\cdot 6H_2O$, Aldrich), and manganese nitrate tetra hydrate ($Mn(NO_3)_2\cdot 4H_2O$, Sigma) salts were dissolved in distilled water, and the total molar concentration of transition metal solutions was fixed at 1 M. The dissolved solution was added into a continuously agitated aqueous citric acid solution, with a molar concentration fixed at 0.2 M. The solution pH was pH 7, which was adjusted using ammonium hydroxide (NH_4OH). The starting solution was atomized using an ultrasonic nebulizer with a resonant frequency of 1.7 MHz. The aerosol stream was introduced into a vertical quartz reactor heated at 500 °C ≤ T ≤ 900 °C. The inner diameter and length of the quartz reactor were 50 and 1200 mm, respectively. The flow rate of air used as a carrier gas was 10 L min^{-1} and the residence time for the transition metal droplets was under 2 s. The prepared $[Ni_{0.4}Co_{0.2}Mn_{0.4}]O_y$ powders were mixed with an excess amount of $LiOH\cdot H_2O$. After the mixture was softly ground, the mixture was heated to 900 °C at a heating rate of 1 °C min^{-1}.

Thermal decomposition behavior of the starting aqueous solution was examined by thermo gravimetric analysis using a Pyris 6 thermal analyzer (TGA, Perkin-Elmer Ltd., USA). The heating/cooling rate was 5 °C min^{-1}. Powder X-ray diffraction (XRD, Rint-2000, Rigaku, Japan) measurement using Cu Kα radiation was employed to identify the crystalline phase of the synthesized material. Particle morphology of the as-prepared and after calcined powders was observed using a scanning electron microscope (SEM, JSM 6400, JEOL, Japan). Differential scanning calorimetry experiments were conducted on $Li[Ni_{0.5}Mn_{0.5}]_{1-x}Co_xO_2$ (x = 0, 0.2) samples charged to 4.5 V (versus metallic Li). The data were acquired using a NETZSCH-TA4 differential scanning calorimeter at a scan rate of 2 °C min^{-1} in the temperature range of RT to 350 °C. Galvanostatic charge/discharge cycling was performed in a 2032-type coin type cell (Hohsen Co. Ltd., Japan). The cell consisted of a cathode and a lithium metal anode separated by porous polypropylene film. The electrode mixture contained of 80% (wt.%) $Li[Ni_{0.4}Co_{0.2}Mn_{0.4}]O_2$ powder, 10% acetylene black, and 10% PVDF binder. The electrolyte solution was 1 M $LiPF_6$ in a mixture of ethylene carbonate (EC) and diethyl carbonate (DEC) in a 1:1 volume ratio (CHEIL Industries Inc., Korea). The cell was assembled in an argon-filled dry box and tested at room temperature (30 °C). The cell was charged and discharged at a current density of 0.2 mA cm^{-2} with cut-off voltages of 2.8–4.4 V (versus Li/Li$^+$).

3. Results and discussion

Thermo gravimetric analysis (TGA) results for starting materials were shown in Fig. 1. All samples has two different weight loss regions. The first weight loss in the temperature range of below 200 °C, which is due to the removal water from each components. The second weight loss in the temperature region of below at 400 °C is related to the decomposition of nitric and chelating agents. The weight loss of the chelating agents, citric acids is almost terminated at 500 °C, indicating that the organic compounds can removed completely

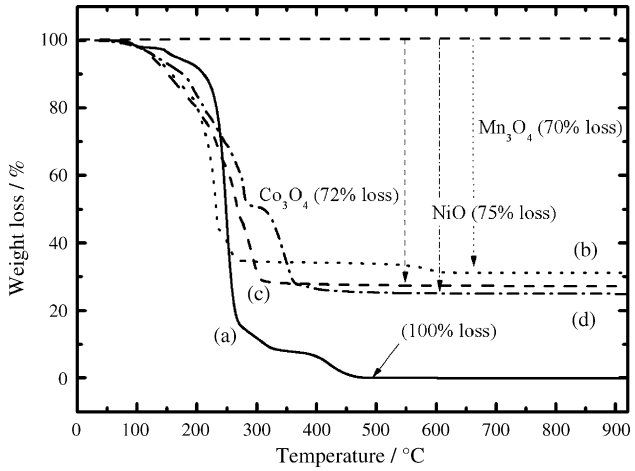

Fig. 1. Thermo gravimetric analysis of the starting materials: (a) citric acid, (b) $Mn(NO_3)_2\cdot 4H_2O$, (c) $Co(NO_3)_2\cdot 6H_2O$, and (d) $Ni(NO_3)\cdot 6H_2O$. All samples were dried in a vacuum oven at 25 °C prior to the thermal analysis and the heating rate was 5 °C min^{-1}.

at temperatures lower than 500 °C. So, we determined that the powders of $[Ni_{0.4}Co_{0.2}Mn_{0.4}]O_y$ can be obtained from the temperature at above 500 °C. However, the weight loss of $Co(NO_3)_2\cdot 6H_2O$, $Mn(NO_3)_2\cdot 4H_2O$ and $Ni(NO_3)_2\cdot 6H_2O$ were approximately 72%, 70%, and 75%, which were might be corresponded Co_3O_4, Mn_3O_4, and NiO, respectively. Moreover, shown in Fig. 2, XRD study is good matched with structure of precursors.

Fig. 2 shows X-ray diffraction (XRD) patterns of the $[Ni_{0.4}Co_{0.2}Mn_{0.4}]O_y$ precursor prepared at various pyrolysis temperatures between 500 and 900 °C. Although the samples prepared at lower pyrolysis temperature (500 and 700 °C) have a very lower crystallinity, all precursors were indexed a mixture of NiO (JCPDS No. 47-1049), Co_3O_4 (JCPDS No. 43-1003), and Mn_3O_4 (JCPDS No. 13-0162). The diffraction peaks were quite broad due to the homogeneous nano-scale mixed particles. However, after firing over 700 °C, the crystallinity well progressed to a cubic spinel M_3O_4 (M = $Ni_{0.4}Co_{0.2}Mn_{0.4}$) structure as can be seen from Fig. 2. From the AAS analysis, the chemical

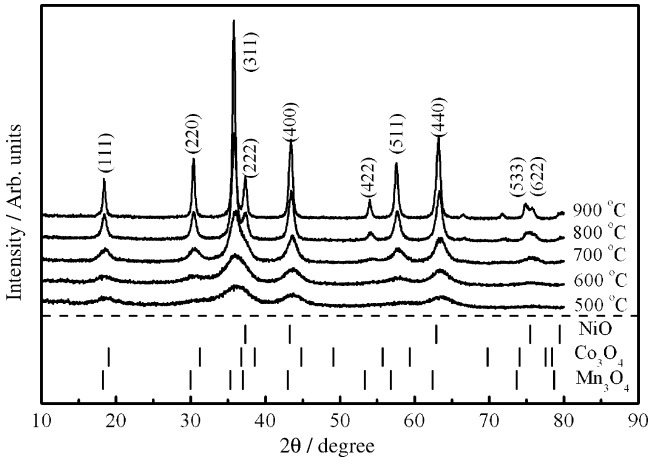

Fig. 2. X-ray diffraction patterns (XRD) of $[Ni_{0.4}Co_{0.2}Mn_{0.4}]O_y$ precursors prepared by various pyrolysis temperatures.

Table 1
The calculated lattice constants, with various pyrolysis temperatures

Pyrolysis temperature (°C)	Space group	*a*-Axis (Å)	Unit volume (Å^3)
500	*Fd*3*m*	8.247(9)	561.09(3)
600	*Fd*3*m*	8.256(8)	562.91(2)
700	*Fd*3*m*	8.282(9)	568.26(5)
800	*Fd*3*m*	8.315(2)	574.94(3)
900	*Fd*3*m*	8.327(4)	577.46(3)

compositions of the prepared powders were determined to be initial compositions. This would be ascribed to the homogeneous precursor, in which cations such as Ni, Co and Mn are uniformly distributed at the atomic scale. Spray pyrolysis is a useful method for the synthesis of high-purity homogenous spherical oxide particles having a narrow size distribution [10–12]. The variation of lattice constants, *a*, and unit cell volume of the prepared powder depending on the preparing temperature are shown in Table 1. The lattice constants were calculated by a least square method from the XRD patterns of Fig. 2. The lattice constants obtained from *Fd*3*m* spinel $(M)_3O_4$ model. By increasing the pyrolysis temperature the lattice constant *a* increased from 8.247(9) Å for 500 °C to 8.327(4) Å for 900 °C, respectively. The higher lattice parameter by the higher temperature calcinations may be caused by high crystallinity, leading to crystal growth.

Fig. 3 shows X-ray diffraction (XRD) patterns of the final $Li[Ni_{0.4}Co_{0.2}Mn_{0.4}]O_2$ powders. All samples could be indexed based on the hexagonal α-$NaFeO_2$ structure with a space group of $R\bar{3}m$ (No. 166). Accordingly, the Li ion is located at the 3b (0, 0, 1/2) site, transition metals at the 3a (0, 0, 0) site, and oxygen is located at the 6c (0, 0, 1/4) site, respectively. At all pyrolysis temperatures a phase-pure layered structure with no impurity phase was observed. The observed diffraction lines show a large integrated peak ratio (0, 0, 3) to (1, 0, 4) and a clear split of the (1, 0, 8) and (1, 1, 0) peaks, which suggests a minimal disorder in the host structure [3]. The calculated lattice parameters of all $Li[Ni_{0.4}Co_{0.2}Mn_{0.4}]O_2$ materials were $a = 2.871(3)$ Å and $c = 14.260(5)$ Å. The measured *c*/*a* ratio is greater than 4.966(5), which indicates a well-ordered layered structure over the range of pyrolysis temperatures used in this study.

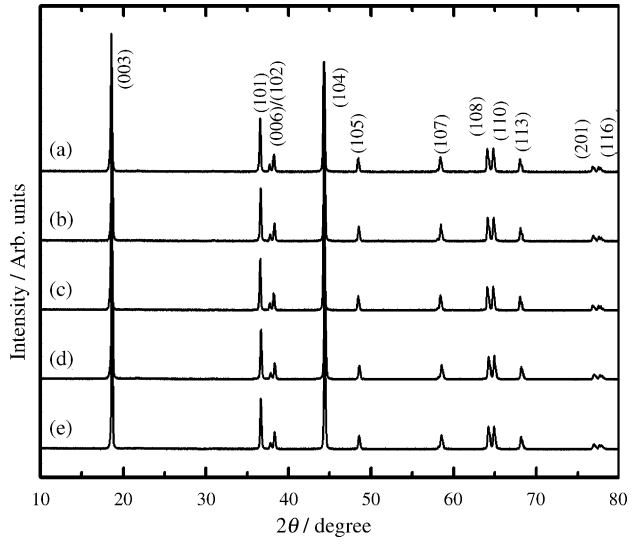

Fig. 3. X-ray diffraction patterns of $Li[Ni_{0.4}Co_{0.2}Mn_{0.4}]O_2$ powders post-calcined at 900 °C with different pyrolysis temperature prepared precursors: (a) 500 °C, (b) 600 °C, (c) 700 °C, (d) 800 °C, and (e) 900 °C.

The scanning electron micrographs (SEM) for the $[Ni_{0.4}Co_{0.2}Mn_{0.4}]O_y$ ($T = 600$ °C) precursor and post-calcined final $Li[Ni_{0.4}Co_{0.2}Mn_{0.4}]O_2$ powders ($T = 900$ °C) are shown in Fig. 4. Fig. 4(a) shows that the as-prepared powder has a spherical morphology with secondary particle sizes of approximately 1–3 μm. Shown in the inset figure is the bright field image of one particle, which consisted of nano-scale primary particles, whose size averaged ~50 nm, for which the observed primary grain size is close to the broadening FWHM of Fig. 2. On the other hand, post-calcined $[Ni_{0.4}Co_{0.2}Mn_{0.4}]O_y$ with $LiOH{\cdot}H_2O$,

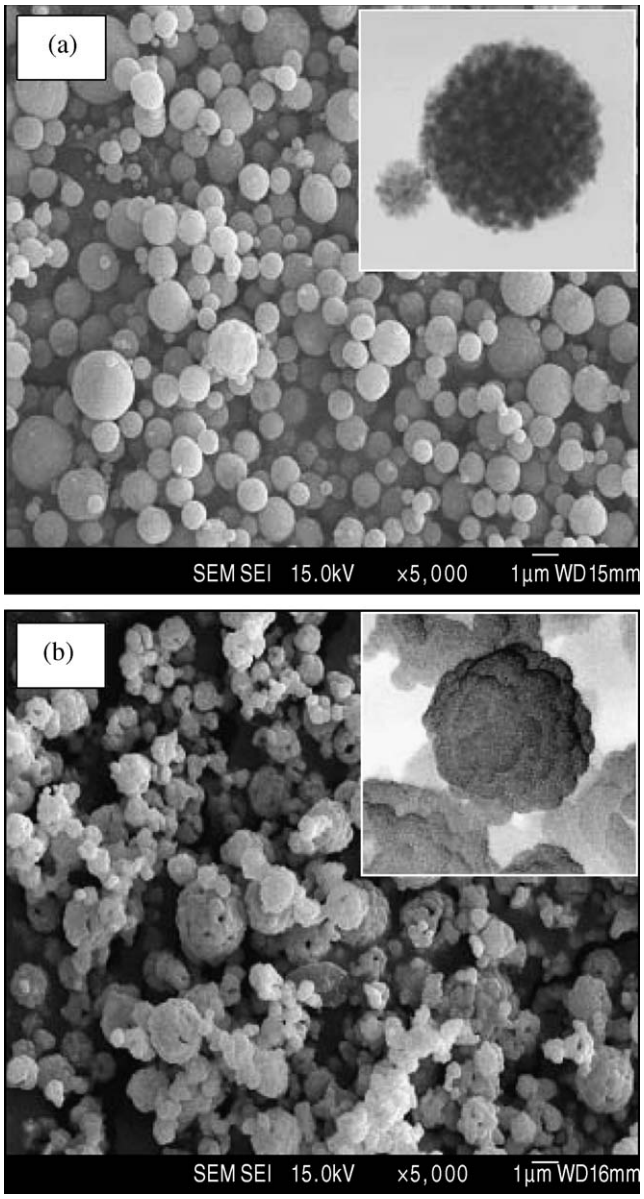

Fig. 4. Scanning electron micrographs (SEM) for (a) $[Ni_{0.4}Co_{0.2}Mn_{0.4}]O_y$ precursors prepared at 600 °C and (b) $Li[Ni_{0.4}Co_{0.2}Mn_{0.4}]O_2$ post-calcined at 900 °C. Inset figures are bright field images at each one particles.

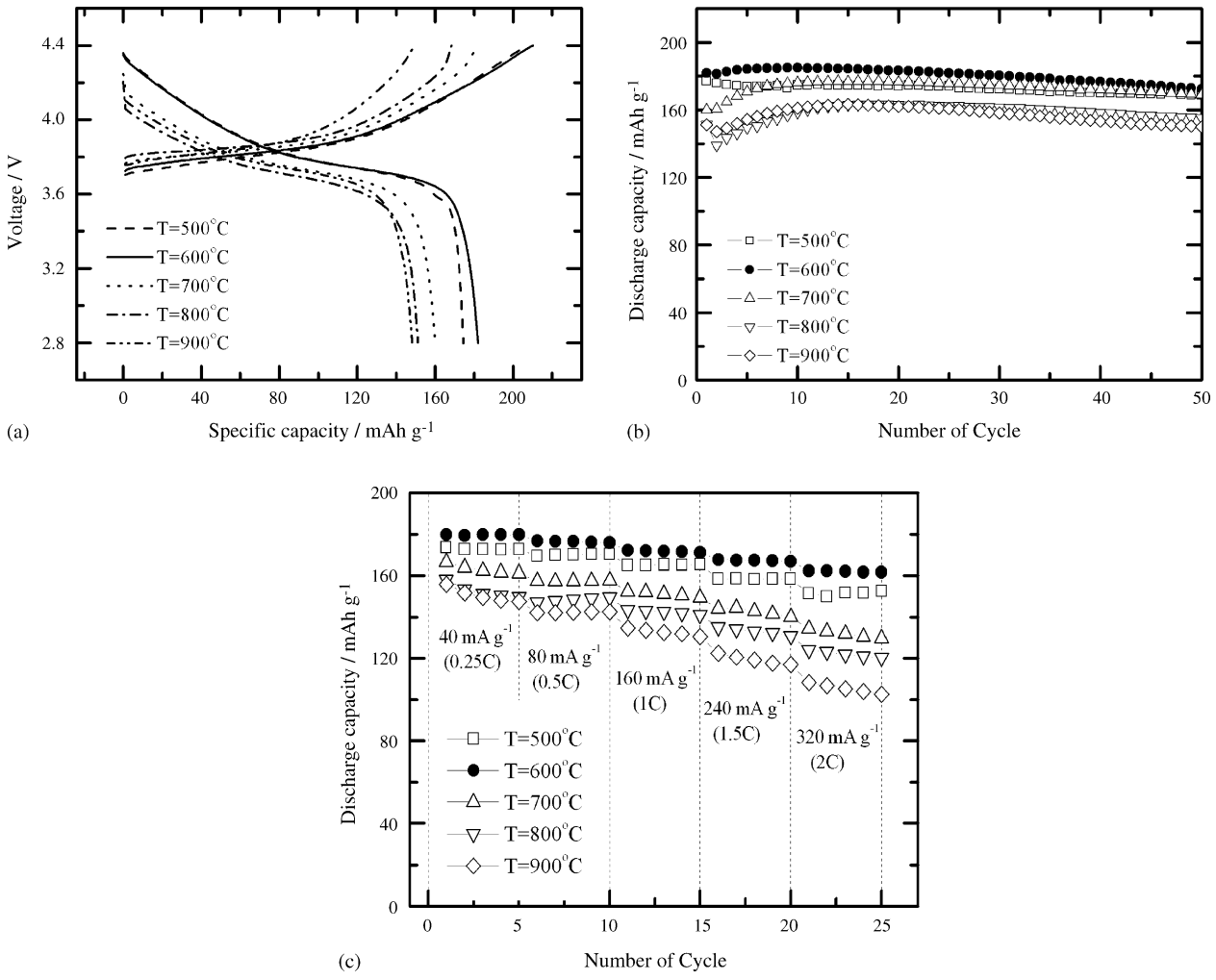

Fig. 5. (a) Charge/discharge voltage profiles, (b) specific discharge capacity vs. number of cycle, and (c) rate capability of Li/Li[$Ni_{0.4}Co_{0.2}Mn_{0.4}$]O_2 cells.

Li[$Ni_{0.4}Co_{0.2}Mn_{0.4}$]O_2 powders have a morphology of a walnut shape, which was 1–3 μm. However, detailed observation of the particle surface shows that Li[$Ni_{0.4}Co_{0.2}Mn_{0.4}$]O_2 powders are composed of lots of sub-micron primary particles. Although, all of SEM images are not shown in this paper, the morphology of post-calcined powders were unchanged with various pyrolysis temperatures.

Fig. 5(a) shows the first charge–discharge voltage profiles for the Li/Li[$Ni_{0.4}Co_{0.2}Mn_{0.4}$]O_2 ($500\,^{\circ}C \le T \le 900\,^{\circ}C$) cells between 2.8 and 4.4 V at a constant current density of 0.2 mA cm^{-2} (20 mA g^{-1}). The charge/discharge curves for all cells were very smooth and unchanged voltage shapes even after 50th cycling, which indicated that layered structure did not change during electrochemical cycling. Particularly, the sample prepared at 600 °C had the highest initial discharge capacity and capacity retention. However, samples prepared at high pyrolysis temperatures ($700\,^{\circ}C \le T \le 900\,^{\circ}C$) show a slightly lower initial discharge capacity, which is attributed to the effect of the pyrolysis temperature on the [$Ni_{0.4}Co_{0.2}Mn_{0.4}$]O_y precursor. The highly crystallized precursor did not allow easy diffusion of lithium in the calcination process. Moreover, starting precursors prepared at high temperature have distinct phase separations for Ni, Co, Mn to NiO, Co_3O_4, Mn_3O_4. Accordingly, precursors prepared at high pyrolysis temperatures showed poor electrochemical properties. Fig. 5(b) shows how the discharge capacity varies with the number of cycles measured at room temperature in the 2.8–4.4 V range with a constant current density of 0.2 mA cm^{-2}. The discharge capacity of 600 °C pyrolysis samples decreases slowly during cycling and remained at 171 mAh g^{-1} after 50 cycles, which is 95% of the initial discharge capacity. Fig. 5(c) shows the various current densities for Li/Li[$Ni_{0.4}Co_{0.2}Mn_{0.4}$]O_2 cells prepared at different pyrolysis temperatures. The cells were charged at a constant current density of 40 mA g^{-1} (0.25 C rates) before at each discharge testing. The discharge capacity slowly decreased with increasing current density and the discharge capacity at a current density of 162 mA g^{-1} (2 C) reached up to 90% compared with 40 mA g^{-1} (0.25 C). The Li[$Ni_{0.4}Co_{0.2}Mn_{0.4}$]O_2 ($T = 600\,^{\circ}C$) electrode showed good rate capability.

Fig. 6 compares the differential scanning calorimetry profiles of Li_y[$Ni_{0.4}Co_{0.2}Mn_{0.4}$]O_2 and Li_y[$Ni_{0.5}Mn_{0.5}$]O_2 samples were charged to 4.5 V. In the presence of the $LiPF_6$ EC:DEC (1:1, v/v) electrolyte, the cobalt free Li[$Ni_{0.5}Mn_{0.5}$]O_2 has one sharp exothermic peak at 280 °C. The thermal decomposition

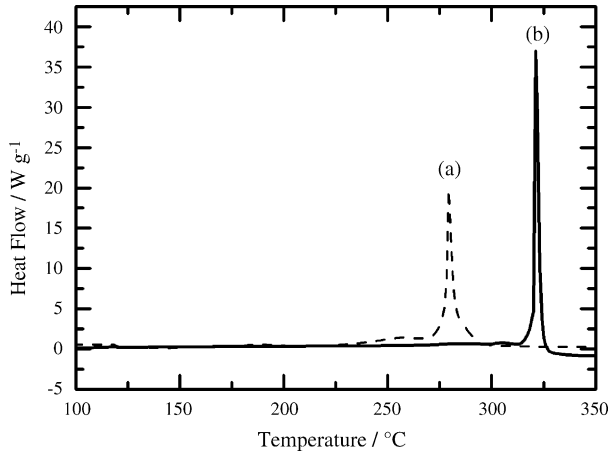

Fig. 6. Differential scanning calorimetry (DSC) profiles of (a) $Li_y[Ni_{0.5}Mn_{0.5}]O_2$ and (b) $Li_y[Ni_{0.4}Co_{0.2}Mn_{0.4}]O_2$ samples charged at 4.5 V vs. Li metal.

properties are affected by the preparation conditions, synthesis method, particle size, distribution, delithiated amount of Li, and different electrolytes. However, the cobalt 0.2 mol substituted $Li[Ni_{0.4}Co_{0.2}Mn_{0.4}]O_2$ material underwent an exothermic reaction with the electrolyte at a much higher temperature of about 320 °C. In spite of the onset of an exothermic peak, however, the peak for decomposition is a little sharper than for the Co-free sample. Thus, these results show that the $Li[Ni_{0.4}Co_{0.2}Mn_{0.4}]O_2$ material possesses superior thermal stability.

4. Conclusion

Spherical morphology mixed transition metal M_3O_4 cubic spinel ($M = Ni_{0.4}Co_{0.2}Mn_{0.4}$) powders were synthesized by an ultrasonic spray pyrolysis method. All precursors were atomic scale and so well mixed and were indexed for NiO (JCPDS No. 47-1049), Co_3O_4 (JCPDS No. 43-1003), and Mn_3O_4 (JCPDS No. 13-0162). However, post-calcined powders with lithium sources exhibited a phase-pure layered structure with a space group of $R\bar{3}m$ (No. 166). The sample prepared at a pyrolysis temperature of 600 °C delivered the high discharge capacity of over 180 mAh g^{-1} between 2.8 and 4.4 V with a capacity retention rate of 0.18 mAh g^{-1} per cycle. Moreover, differential scanning calorimetry results revealed that the $Li[Ni_{0.4}Co_{0.2}Mn_{0.4}]O_2$ electrode has a better thermal safety characteristic than cobalt free $Li[Ni_{0.5}Mn_{0.5}]O_2$ electrodes. Consequently, $Li[Ni_{0.4}Co_{0.2}Mn_{0.4}]O_2$ materials are better candidates for the cathode material in rechargeable lithium-ion batteries.

Acknowledgment

This work was supported by the Ministry of Information and Communications, Korea, under the Information Technology Research Center (ITRC) Support Program.

References

[1] J.R. Dahn, E.W. Fuller, M. Obrovac, U. von Sacken, Sloid State Ionics 69 (1994) 265.
[2] H. Arai, Y. Sakurai, J. Power Sources 81/82 (1999) 401.
[3] T. Ohzuku, A. Ueda, M. Kouguchi, J. Electrochem. Soc. 142 (1995) 4033.
[4] B. Ammundsen, J. Paulsen, Adv. Mat. 13 (2001) 943.
[5] G. Vitins, K. West, J. Electrochem. Soc. 144 (1997) 2587.
[6] Y.-I. Jang, B. Huang, Y.-M. Chiang, D.R. Sadoway, Electrochem. Solid State Lett. 1 (1998) 13.
[7] T. Ohzuku, Y. Makimura, Chem. Lett. 7 (2001) 642.
[8] K.M. Shaju, G.V. Subba Rao, B.V.R. Chowdari, Electrochim. Acta 48 (2002) 145.
[9] S.W. Oh, S.-H. Park, C.-W. Park, Y.-K. Sun, Solid State Ionics 171 (2004) 167.
[10] H. Xu, L. Gao, H.C. Gu, D.S. Yan, J. Am. Ceram. Soc. 85 (2002) 139.
[11] Y.C. Kang, S.B. Park, J. Mater. Sci. Lett. 16 (1997) 131.
[12] I. Taniguch, Mater. Chem. Phys. 92 (2005) 172.